КОНДЕНСИРОВАННЫЕ СРЕДЫ И МЕЖФАЗНЫЕ ГРАНИЦЫ, ТОМ 19, № 3, С. 341–351

UDC 536.7:546.78

ANALYSIS OF THE STATE OF ISOPOLYNIOBOTUNGSTATE ANIONS (Nb:W = 3:3) AND THEIR SYNTHESIS FROM AQUEOUS SOLUTIONS

© 2017 S. M. Vavilova[1], M. A. Kryuchkov[2], V. V. Ignatyeva[3], E. E. Belousova[4]

[1]Voronezh State Medical University named after N.N. Burdenko, 10 Studencheskaya str., 394036 Voronezh, Russia
e-mail: e-mail: svavilova@mail.ru
*[2]Department of Chemistry, McGill University, Montreal, Quebec, Canada**
e-mail: maks_ne@yahoo.com
[3]M. Gorky Donetsk National Medical University, 16 Av. Illicha, 83003 Donetsk, Donetsk People's Republic
e-mail: ignatyevavictoriya@gmail.com
[4]Donetsk National University, 24 Universitetskaya str., 83001 Donetsk, Donetsk People's Republic

Received 20.07.2017

Abstract. The formation of complexes in the system $Nb_6O_{19}^{8-}$–WO_4^{2-}–H^+–H_2O, where Nb:W = 3:3 and c^0_{Nb+W} = 10, 5, 2.5 and 1 mmol/L, was studied by pH–complexonometric titration. Using computer modeling of the processes of complexes formation (CLINP 2.1 software), concentrational constants of the mixed isopolyniobotungstate anions formation were obtained ($Z = \frac{c^0_{H^+}}{c^0_{Nb+W}} = 0 - 3.0$, background electrolyte is NaCl) and their distribution diagrams were built. The thermodynamic constants of $H_xNb_3W_3O_{19}^{(5-x)-}$ (x = 0–3) formation were calculated, and it was shown that the formation of these anions takes place only after the polycondensation of the initial orthotungstate anions. Calcium and Thallium salts ($Ca_{1.5}H_2Nb_3W_3O_{19}\cdot 12H_2O$ and $Tl_{5-x}H_xNb_3W_3O_{19}\cdot nH_2O$, respectively, x = 1–3) were prepared and characterized by X–ray spectral analysis, scanning electron microscopy, and IR-spectroscopy.

Keywords: polyoxometalates, isopolyanion, isopolyniobotungstate, Lindqvist anion, modeling complex formation in solution.

INTRODUCTION

Isopolyniobotungstate anion (IPNTA) salts of the fifth and sixth periods of the Periodic Table [1] as well as their heteropoly compounds possess catalytic [2–6] and antivirus activity [7]. IPNTA complexes with d- and f-elements are perspective proton conductors [8], solid state ion conductors [9, 10] and materials with unusual optical properties [11, 12]. Moreover, materials based on IPNTA and silicon can potentially be used as sorbents []. The majority of the published works on IPNTA are dedicated to the application of their salts as a starting material in the synthesis of the new coordination compounds [13–16], whereas optimization of the synthetic procedures and qualitative and quantitative characterization of IPNTA in solution are being paid much less attention. However, these data is needed to obtain more active protonated forms of IPNTA and to improve the quality of the obtained salts, especially for biomedical purposes.

The aim of this report was to study the formation of the complexes of $H_xNb_3W_3O_{19}^{(5-x)-}$ (x = 0–3) in the system $Nb_6O_{19}^{8-}$–WO_4^{2-}–H^+–H_2O with Nb:W = 3:3 using pH-potentiometric titration; and to determine the Z-regions of existence for all the IPNTAs involved. The latter allowed preparing the targeted compounds $H_xNb_3W_3O_{19}^{(5-x)-}$ (x = 0–3) with Nb:W = 3:3 that do not contain any impurities of other IPNTA. To achieve this, despite the commonly used procedure [17], solutions of hydrochloric acid, sodium orthotungstate and potassium hexaniobate in stoichiometric ratio were used instead. Such procedure allowed avoiding the unwanted excess of potassium hexaniobate as well as utilization of hydrogen peroxide for its stabilization, therefore the final product was not contaminated with niobium peroxide derivatives.

* Present address: BioAstra Technologies Inc., 6100 Av. Royalmount, Montreal, QC, Canada H4P 2R2.

EXPERIMENTAL

The studies of the complexes formation in the system $Nb_6O_{19}^{8-}$–WO_4^{2-}–H^+–H_2O were carried out by pH-complexonometric titration at 25±0.1 °C, using I-500 (Aquilon, Russia) ionometer. Indicator electrode was hydrogen-ion selective glass electrode ESL 63-07 Sr (Belarus) with isopotential point pH_i = 7.00 and E_i = –25±10 mV, auxiliary electrode EVL-1M3 was silver chloride electrode (Ag/AgCl, sol. KCl, saturated) with the potential of 202±2 mV, according to standard hydrogen electrode. Calibration and preciseness of the readings were controlled by the series of standard buffer solutions, prepared according to Bates [18]. In the systems under investigation the overall concentrations of Nb+W (c^0_{Nb+W}) were 10, 5, 2.5 and 1 mmol/L and c_{Nb}: c_W = 3:3.

The acidity of the systems during titration $Z = \frac{c^0_{H^+}}{c^0_{Nb+W}}$ ($c^0_{H^+}$ is the overall concentration of acid and c^0_{Nb+W} is the overall concentration of niobium and tungsten in solution) was controlled by the amount of the acid being added with step ΔZ = 0.02 within the interval Z = 0÷2. The ionic strength was created by the background electrolyte (NaCl) and was varied within I = 0.01÷1.00.

The initial solutions were prepared from solids or concentrated solutions using distilled water, purified from CO_2. Potassium haxaniobate solution was prepared by dissolving of freshly prepared salt $4K_2O{\cdot}3Nb_2O_5{\cdot}12H_2O$. It was prepared by annealing of Nb_2O_5 with 5-fold excess of KOH, followed by thorough washing with the distilled water and double recrystallization from acetone. Sodium tungstate and sodium chloride solutions were prepared by dissolving of solids in water and the solution of hydrochloric acid was prepared by diluting of the concentrated (10M) solution. The precise concentrations of initial solutions were determined according to chemical analysis data: the contents of tungsten and niobium were determined gravimetrically (gravimetric forms WO_3 and Nb_2O_5, $\delta \le \pm 0.5\%$), hydrochloric acid was standardized by titration of $Na_2B_4O_7{\cdot}10H_2O$ with methyl red indicator, $\delta \le \pm 0.8\%$.

For interpretation of experimental data, the mathematical modeling using CLINP 2.1 software was utilized [19]. Each model was evaluated for consistency with the experimental data. The models were checked for excessiveness (Jacobi matrix) and adequateness (the main criterion is $\chi^2_{exp} < \chi^2_{f,\alpha=0.05}$) to the experimental data. Indirect indication of the adequateness of the created models was the coherence of the experimental and calculated titration curves at each point within $\left|pH_i^{calcd} - pH_i^{exp}\right| \le 0.12$.

The result of mathematical modeling was the determination of concentrational formation constants ($\lg K_C$) for the anions in solution. Based on the obtained values, thermodynamic formation constants $\lg K°$ for individual IPNTA were calculated by Pitzer method [21–22] by approximation of the dependence of concentrational constants $\lg K_C$ on the ionic strength $\lg K_C(I)$ to its zero value I→0.

Calculation of the formation constants allowed building of the distribution diagrams and determination of the regions of predominant formation of the desired IPNTA. Furthermore, in these regions at fixed Z values the solid phase was precipitated, which was either individual salt with $H_xNb_3W_3O_{19}^{(5-x)-}$ (x = 0–3) anion or the mixture of salts with varying x value. To determine the phase anion, hydrochloric acid was added to the mixture of initial solutions of potassium hexaniobate and sodium orthotungstate (Nb:W = 3:3) to reach Z = 1.00 and Z = 1.18, and then 1.5–fold excess of thallium (I) or calcium (II) nitrate was added dropwise at rigorous stirring. The obtained suspension was stirred for 5 hours, and then the white precipitation was isolated by filtration, washed with cold water and dried in the air till constant mass.

Studying of the surface morphology of the prepared salts and their energy-dispersive X-ray spectral microanalysis (EDX) were performed on JSM 6490 LV scanning electron microscopy (SEM) instrument with lanthanum hexaboride cathode and accelerating voltage of 10–20 kV. Phase elemental analysis was carried out in backscattered electron imaging (BEI) regime, and surface analysis was done in secondary electron imaging (SEI) regime.

Chemical analysis of the solid phase was carried out as follows. The contents of niobium and tungsten were determined gravimetrically (gravimetric forms WO_3 and Nb_2O_5, $\delta \le \pm 0.5\%$); the contents of the crystalline water was determined gravimetrically (sample annealing at 500 °C until constant mass, $\delta \le \pm 0.5\%$); the contents of Tl_2O was determined by complexonometric titration (reverse titration of Trilon B by $ZnCl_2$, xylenol orange indicator, $\delta \le \pm 0.8\%$); the contents of calcium were determined by complexonometric titration (direct titration of the solution with pH = 8 by Trilon B, methylthymol blue indicator, $\delta \le \pm 0.8\%$). Anions in the obtained salts were identified by Fourier-transformed infrared spectroscopy (FTIR) using Tensor 27 (Bruker Optics) in the region of 400–4000 cm^{-1} in KBr pellets. Low-resolved regions of the spectra were clarified by Gauss components extraction (using Peak Fit plug–in

for Origin 8.0 software) until R = 0.999 for experimental and clarified spectra.

RESULTS AND DISCUSSION

For systems $Nb_6O_{19}^{8-}$–WO_4^{2-}–H^+–H_2O with the overall concentration c^0_{Nb+W} = 10, 5, 2.5 and 1 mmol/L and Nb:W = 3:3 pH-potentiometric titration was carried out at ionic strengths I = 0.01÷0.30 created by NaCl. It turned out that general behaviour of the titration curves at any ionic strength and given concentration is practically the same. Thus, for further discussion, only one typical curve for each concentration will be shown (Fig. 1).

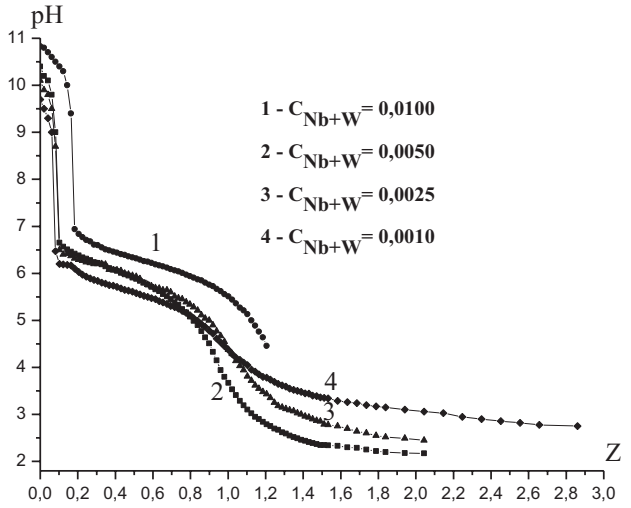

Fig. 1. pH-potentiometric curves pH = *f*(*Z*) for the system $Nb_6O_{19}^{8-}$–WO_4^{2-}–H^+–H_2O at different c^0_{Nb+W} and I = 0.10 mol/L

All the titration curves display two characteristic pH gaps that most probably correspond to the protonation of niobium anions and polycondensation of tungsten anions. It is worth mentioning that, with the decrease of c^0_{Nb+W}, pH gaps that correspond to higher *Z* become less vivid, and the range of homogeneity for each system is not the same for different concentrations and decreases as c^0_{Nb+W} increases.

Using calculated theoretical values of Z_{theor} for the formation of various polyanionic forms of tungsten and niobium (polyanionic forms of tungsten, niobium and IPNTA), one can select particular reactions that can proceed at fixed *Z* intervals, as depicted in titration curves in Fig. 1. Thus, the reactions of protonation of the initial hexaniobate-anion belong to the region *Z* < 0.3:

$$xH^+ + Nb_6O_{19}^{8-} \leftrightarrow H_xNb_6O_{19}^{(8-x)-},\ x = 1\div3.$$

The region 0.7 < *Z* < 1.3 can be described by the processes of polycondensation of the initial tungstate-anion and IPNTA formation:

$$7WO_4^{2-} + 9H^+ \leftrightarrow HW_7O_{24}^{5-} + 4H_2O \quad Z = 0.64,$$

$$12WO_4^{2-} + 18H^+ \leftrightarrow W_{12}O_{38}(OH)_2^{6-} + 4H_2O \quad Z = 0.75,$$

$$10WO_4^{2-} + 16H^+ \leftrightarrow W_{10}O_{32}^{4-} + 8H_2O \quad Z = 0.80,$$

$$10WO_4^{2-} + 17H^+ \leftrightarrow HW_{10}O_{32}^{3-} + 8H_2O \quad Z = 0.85,$$

$$Nb_6O_{19}^{8-} + 6WO_4^{2-} + 10H^+ \leftrightarrow 2Nb_3W_3O_{19}^{5-} + 5H_2O \quad Z = 0.83,$$

$$Nb_6O_{19}^{8-} + 6WO_4^{2-} + 12H^+ \leftrightarrow 2HNb_3W_3O_{19}^{4-} + 5H_2O \quad Z = 1.00,$$

$$Nb_6O_{19}^{8-} + 6WO_4^{2-} + 14H^+ \leftrightarrow 2H_2Nb_3W_3O_{19}^{3-} + 5H_2O \quad Z = 1.17,$$

$$Nb_6O_{19}^{8-} + 6WO_4^{2-} + 16H^+ \leftrightarrow 2H_3Nb_3W_3O_{19}^{2-} + 5H_2O \quad Z = 1.33.$$

However, it is impossible to determine whether particular or all the reactions take place. Such an ambiguity in treated experimental data makes it impossible the precise explanation of gaps in titration curves pH = *f*(*Z*), and thus does not allow proposing the schemes of interionic transformations as well as calculating of formation constants of IPNTA. That is why mathematical modeling (CLINP 2.1 software) was used to find the models that adequately describe the formation of complexes in studied systems.

As mentioned above, within one concentration the general behaviour of pH = *f*(*Z*) does not depend on I, so the detailed description of pH-potentiometric data can be exemplified by one concentration (c^0_{Nb+W} = 1 mmol/L) and one ionic strength (I = 0.5 mol/L). Notably, at this concentration both pH gaps are well defined within relatively big region of homogeneity.

First of all, the *Model 1* that contains only IPNTA of $H_xNb_3W_3O_{19}^{(5-x)-}$ (*x* = 0–4) was tested. Experimental and calculated curves overlap (ΔpH ≤ 0.12) only in the region of *Z* > 1, whereas at lower *Z* the experimental curve is not described at all (Fig. 2.1). Also, the main criterion of adequacy for *Model 1* ($\chi^2_{exp} = 1793 \gg \chi^2_{f,\,\alpha=0.05} = 119$) is unsatisfactory. Stepwise introduction of isopolytungstate-anions (IPTA) into *Model 1* allowed improving of experimental and calculated curves overlapping in a small region of middle *Z* values. Although it is not so vivid in Fig. 2.2, the criterion $\chi^2_{exp} = 1785 \gg \chi^2_{f,\,\alpha=0.05} = 119$ somewhat improved. Besides, from all the tried IPTA, only $W_6O_{20}(OH)_2^{6-}$ and $HW_7O_{24}^{5-}$ lead to χ^2_{exp} improvement, and so they were left in *Model 2*. The region of low *Z* values became described after introduction of the protonated form of the initial $Nb_6O_{19}^{8-}$ into the model (Fig. 2.3). Before the final model was created,

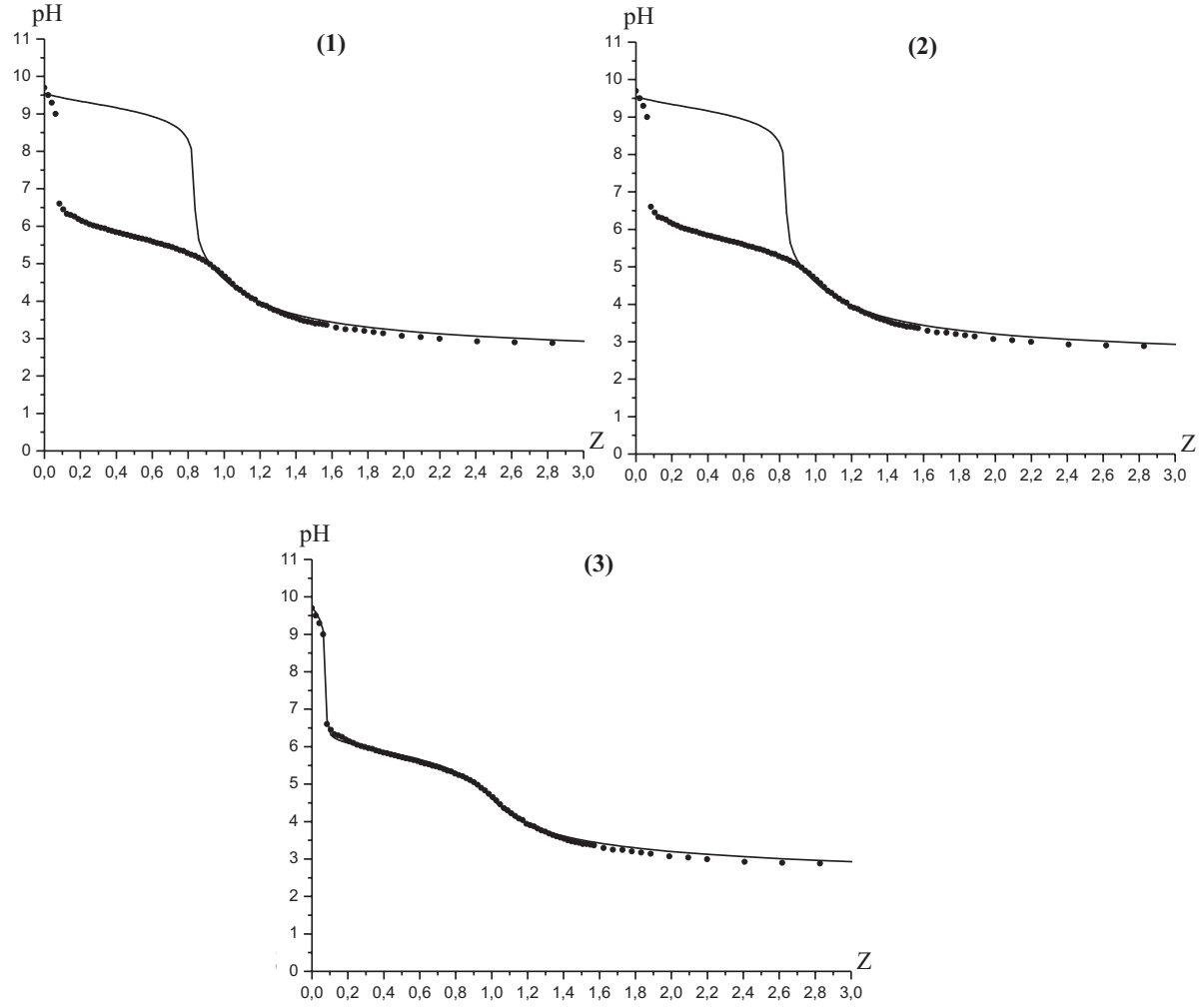

Fig. 2. Mathematical modeling steps for the system $Nb_6O_{19}^{8-}$–WO_4^{2-}–H^+–H_2O with Nb:W = 3:3, c^0_{Nb+W} = 1 mmol/L and I = 0.5 mol/L. ····· – experimental; —— – calculated. (1) – ***Model 1***: WO_4^{2-}, $Nb_6O_{19}^{8-}$, $Nb_3W_3O_{19}^{5-}$, $HNb_3W_3O_{19}^{4-}$, $H_2Nb_3W_3O_{19}^{3-}$, $H_3Nb_3W_3O_{19}^{2-}$, $H_4Nb_3W_3O_{19}^{-}$; (2) – ***Model 2***: WO_4^{2-}, $Nb_6O_{19}^{8-}$, $Nb_3W_3O_{19}^{5-}$, $HNb_3W_3O_{19}^{4-}$, $H_2Nb_3W_3O_{19}^{3-}$, $H_3Nb_3W_3O_{19}^{2-}$, $H_4Nb_3W_3O_{19}^{-}$, $HW_7O_{24}^{5-}$, $W_6O_{20}(OH)_2^{6-}$; (3) – ***Model 3***: WO_4^{2-}, $Nb_6O_{19}^{8-}$, $Nb_3W_3O_{19}^{5-}$, $HNb_3W_3O_{19}^{4-}$, $H_2Nb_3W_3O_{19}^{3-}$, $HW_7O_{24}^{5-}$, $W_6O_{20}(OH)_2^{6-}$, $HNb_6O_{19}^{7-}$

we eliminated those particles whose values in the Jacob matrix were less than 10^{-4}–10^{-6}, indicating the excessiveness of the model. Finally, *Model 3* was derived containing equilibrium transformations between $H_xNb_3W_3O_{19}^{(5-x)-}$ (x = 0–2), $HNb_6O_{19}^{7-}$, $W_6O_{20}(OH)_2^{6-}$ and $HW_7O_{24}^{5-}$. *Model 3* adequately describe the titration curve along the entire studied Z interval ($\chi^2_{exp} = 109 < \chi^2_{f,\alpha=0.05} = 120$). Other particles combinations in models showed less adequacy than *Model 3*, thus it was further used as the basic model.

Since the protonation of hexaniobate-anions and polycondensation of orthotungstate-anions are well studied and their formation constants have been determined, we used those literature values for our calculations. Thus, for $HNb_6O_{19}^{7-}$ –log K = 11.9 (Z_{theor} = 0.03) [23]; for $W_6O_{20}(OH)_2^{6-}$ – log K = 50.41 (Z_{theor} = 0.83); for $HW_7O_{24}^{5-}$ –logK = 70.70 (Z_{theor} = 1.07) [24]. Concentrational formation constants for all the IPNTA present in our models were not known, so they were calculated (Table 1).

We found that the model describing the processes that take place at acidification of the systems with c^0_{Nb+W} = 5 and 2.5 mmol/L is the same as for more diluted solution (1 mmol/L). The peculiarity of the system with c^0_{Nb+W} = 10 mmol/L if compared to more diluted solutions is that non-protonated anion $Nb_3W_3O_{19}^{5-}$ is absent, but highly-protonated form $H_3Nb_3W_3O_{19}^{2-}$ is present.

The obtained full set of $logK_C$'s allowed calculating the concentration of anions and building of the distribution diagrams of ionic forms [molar content of the anion (α) as a function of acidity (Z)] for all the studied systems. As the contents of the model does

Table 1. Log K_C values for $H_xNb_3W_3O_{19}^{(5-x)-}$ at c^0_{Nb+W} = 10, 5, 2.5 and 1 mmol/L and varied ionic strengths I

	lgK_C (S*) at ionic strength, I, mol/L								
	c^0_{Nb+W} = 10 mmol/L								
	0.1		0.15		0.2		0.25		0.3
$HNb_3W_3O_{19}^{4-}$	49.08 (0.03)		49.62 (0.03)		49.05 (0.04)		49.77 (0.03)		48.83 (0.09)
$H_2Nb_3W_3O_{19}^{3-}$	54.23 (0.03)		54.62 (0.04)		53.95 (0.04)		54.62 (0.04)		53.71 (0.10)
$H_3Nb_3W_3O_{19}^{3-}$	58.17 (0.05)		58.67 (0.06)		57.56 (0.07)		58.64 (0.06)		57.15 (0.15)
	c^0_{Nb+W} 5 mmol/L								
	0.05	0.06	0.08	0.09	0.10	0.11	0.12	0.13	0,14
$Nb_3W_3O_{19}^{3-}$	39.81 (0.04)	39.89 (0.04)	39.57 (0.06)	40.25 (0.06)	39.78 (0.04)	39.80 (0.04)	39.69 (0.04)	40.09 (0.02)	39,81 (0,03)
$HNb_3W_3O_{19}^{4-}$	43.74 (0.04)	43.81 (0.04)	43.51 (0.05)	44.30 (0.06)	43.84 (0.03)	43.79 (0.03)	43.68 (0.04)	44.48 (0.02)	43,74 (0,03)
	c^0_{Nb+W} 2.5 mmol/L								
	0.03	0.04	0.05	0.06	0.07	0.08	0.10	0.12	0.14
$Nb_3W_3O_{19}^{3-}$	40.77 (0.05)	40.63 (0.05)	40.40 (0.07)	40.29 (0.07)	40.58 (0.07)	40.09 (0.10)	40.69 (0.07)	40.23 (0.09)	40,96 (0,08)
$HNb_3W_3O_{19}^{4-}$	45.46 (0.05)	45.29 (0.06)	45.04 (0.06)	44.96 (0.07)	45.52 (0.07)	44.84 (0.09)	45.61 (0.07)	44.99 (0.09)	45,36 (0,09)
	c^0_{Nb+W} 1 mmol/L								
	0.01	0.02	0.03	0.04	0.05	0.06	0.08	0.10	
$Nb_3W_3O_{19}^{3-}$	40.47 (0.06)	40.53 (0.06)	40.60 (0.06)	40.68 (0.06)	40.96 (0.07)	40.56 (0.07)	40.71 (0.07)	40.20 (0.08)	
$HNb_3W_3O_{19}^{4-}$	45.38 (0.06)	45.64 (0.05)	45.68 (0.06)	45.73 (0.06)	46.16 (0.07)	45.78 (0.06)	45.86 (0.07)	45.44 (0.07)	
$H_2Nb_3W_3O_{19}^{3-}$	–	49.56 (0.07)	49.61 (0.07)	49.68 (0.06)	49.89 (0.09)	49.24 (0.11)	49.37 (0.11)	–	

* – *S* is the root mean square deviation of log K_C.

not change much within particular concentration, the general tendency can be visualized by diagrams for lowest and highest concentrations, because namely them differ most by the degree of $H_xNb_3W_3O_{19}^{(5-x)-}$ anion protonation (Fig. 3).

Thermodynamic formation constants of IPNTA (logK°, Table 2) were calculated by Pitzer method using averaged $logK_C$ values for different c^0_{Nb+W} and same ionic strength (Table 1). This allowed analyzing the obtained distribution diagrams taking into account the free Gibbs energies ($\Delta G°_{react} = -RT \log K°$) of reactions of polyanions formation.

Noteworthy, processes of IPNTA formation at Nb:W = 3:3 differs from ones in the systems with higher tungsten content (Nb:W = 1:5 [25] and 2:4 [26]). IPNTA with the Nb:W ratio prescribed by the stoichiometry of the initial solutions form immediately and without the formation of other IPNTA with higher niobium content, i.e. $H_xNb_aW_{6-a}O_{19}^{(2+a-x)-}$ ($a \geq 4$). Thus, $H_xNb_3W_3O_{19}^{(5-x)-}$ ($x = 0, 1$) are the products of interaction between protonated hexaniobate-anions $H_xNb_6O_{19}^{(8-x)-}$ ($x = 1, 2$) and polyforms of tungsten $W_6O_{20}(OH)_2^{6-}$ and $HW_7O_{24}^{5-}$ at Nb:W = 1:1. From the above, the desired IPNTA can be obtained via two routes that differ by the nature of isopolyniobate anion (IPNA).

In the first route the initial ions are hexatungstate anion:

$$HNb_6O_{19}^{7-} + W_6O_{20}(OH)_2^{6-} + 3H^+ \rightarrow$$
$$\rightarrow 2Nb_3W_3O_{19}^{5-} + 3H_2O$$
$$\Delta G^0_{react} = -105.5 \text{ (kJ/mol)},$$

$$H_2Nb_6O_{19}^{6-} + W_6O_{20}(OH)_2^{6-} + 4H^+ \rightarrow$$
$$\rightarrow 2HNb_3W_3O_{19}^{4-} + 3H_2O$$
$$\Delta G^0_{react} = -110.8 \text{ (kJ/mol)}.$$

In the second route with the acidity $Z > 0.8$ initially hexatungstate-anion transforms into heptatungstate:

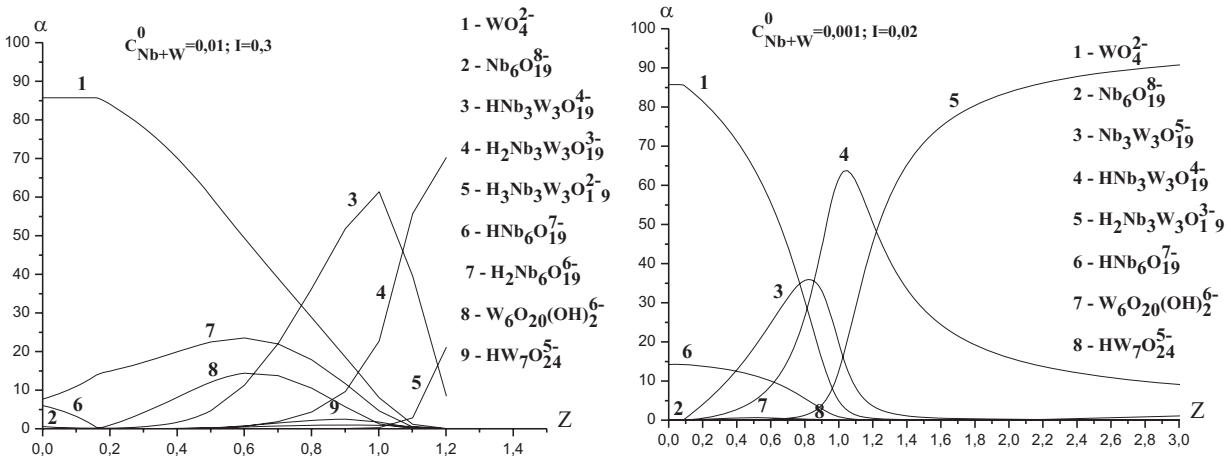

Fig. 3. Distribution diagrams of anions in the system $Nb_6O_{19}^{8-}$–WO_4^{2-}–H^+–H_2O and Nb:W = 3:3 at different c^0_{Nb+W} (mol/L) and ionic strength *I*, mol/L

Table 2. Averaged log K_C values at different ionic strength *I*, and log K° values for $H_xNb_3W_3O_{19}^{(5-x)-}$

I, mol/L	log K_C (S*)			
	$Nb_3W_3O_{19}^{5-}$	$HNb_3W_3O_{19}^{4-}$	$H_2Nb_3W_3O_{19}^{3-}$	$H_3Nb_3W_3O_{19}^{2-}$
0,01	40.47 (0.06)	45.38 (0.06)	–	–
0.02	40.53 (0.06)	45.64 (0.05)	49.56 (0.07)	–
0.03	40.69 (0.05)	45.57 (0.05)	49.61 (0.07)	–
0.04	40.65 (0.06)	45.38 (0.06)	49.68 (0.06)	–
0.05	40.39 (0.06)	45.08 (0.05)	49.89 (0.09)	–
0.06	40.25 (0.06)	45.85 (0.05)	49.24 (0.11)	–
0.07	40.58 (0.07)	45.52 (0.07)	–	–
0.08	40.12 (0.07)	44.73 (0.07)	49.37 (0.11)	–
0.09	40.25 (0.06)	44.30 (0.06)	–	–
0.10	40.22 (0.06)	44.96 (0.06)	54.23 (0.03)	58.07 (0.05)
0.11	39.80 (0.04)	43.79 (0.03)	–	–
0.12	39.96 (0.06)	44.34 (0.05)	–	–
0.13	40.09 (0.02)	44.48(0.02)	–	–
0.14	40.39 (0.05)	44.55 (0.08)	–	–
0.15	–	49.62 (0.03)	54.62 (0.04)	58.67 (0.06)
0.20	–	49.05 (0.04)	53.95 (0.04)	57.56 (0.07)
0.25	–	49.77 (0.03)	54.62 (0.04)	58.64 (0.06)
0.30	–	48.83 (0.09)	53.71 (0.10)	57.10 (0.15)
lgK⁰	**41.62 ± 0.11**	**48.05 ± 0.67**	**54.28 ± 0.48**	**60.47 ± 0.95**

* – *S* is the root mean square deviation of log K_C.

$$7/6W_6O_{20}(OH)_2^{6-} + 2H^+ \rightarrow HW_7O_{24}^{5-} + 4H_2O$$
$$\Delta G^0_{react} = -79.6 \text{ (kJ/mol)}$$

and then the product prescribed by the stoichiometry of the initial solutions forms with the participation of $HW_7O_{24}^{5-}$:

$$HNb_6O_{19}^{7-} + 0.86HW_7O_{24}^{5-} + 1.42H^+ \rightarrow$$
$$\rightarrow 2Nb_3W_3O_{19}^{5-} + 1.64H_2O$$
$$\Delta G^0_{react} = -46.29 \text{ (kJ/mol)},$$

$$H_2Nb_6O_{19}^{6-} + 0.86HW_7O_{24}^{5-} + 2.42H^+ \rightarrow$$
$$\rightarrow 2HNb_3W_3O_{19}^{4-} + 1.64H_2O$$
$$\Delta G^0_{react} = -14.89 \text{ (kJ/mol)}.$$

Negative values of ΔG^0_{react} indicate the possibility that both routes can proceed. At lower acidity values ($Z < 0.8$) $W_6O_{20}(OH)_2^{6-}$ participates in thermodynamically more feasible reactions with the formation of $H_xNb_3W_3O_{19}^{(5-x)-}$ and $HW_7O_{24}^{5-}$. At higher acidity ($Z > 0.8$), when concentration of $HW_7O_{24}^{5-}$ is high enough, the formation of IPNTA proceeds via two routes, i.e. from hexa- and heptatungstate anions.

Further increase of acidity of the systems leads to protonation of the desired anion:

$$Nb_3W_3O_{19}^{5-} + H^+ \rightarrow HNb_3W_3O_{19}^{4-}$$
$$\Delta G^0_{react} = -36.71 \text{ (kJ/mol)},$$

$$HNb_3W_3O_{19}^{4-} + H^+ \rightarrow H_2Nb_3W_3O_{19}^{3-}$$
$$\Delta G^0_{react} = -35.34 \text{ (kJ/mol)},$$

$$H_2Nb_3W_3O_{19}^{3-} + H^+ \rightarrow H_3Nb_3W_3O_{19}^{2-}$$
$$\Delta G^0_{react} = -35.34 \text{ (kJ/mol)}.$$

Interestingly, when titrated solutions were diluted till $c^0_{Nb+W} \leq 2.5$ mmol/L, first, hydrolysis of the initial $Nb_6O_{19}^{8-}$ into $HNb_6O_{19}^{7-}$ at $Z = 0$ proceeds to more extent, and protonation of $Nb_3W_3O_{19}^{5-}$ takes place at x values from 0 to 2 to give $H_xNb_3W_3O_{19}^{(5-x)-}$. Second, distribution diagrams of the ionic forms do not reflect quantitative accumulation of the tungsten polyforms $W_6O_{20}(OH)_2^{6-}$ and $HW_7O_{24}^{5-}$ in solution. At the same time, their absence makes the correspondence of the modeling results with experimental data much worse, thus requiring to keep $W_6O_{20}(OH)_2^{6-}$ and $HW_7O_{24}^{5-}$ in the model. In our opinion, the absence of IPTA can be explained by their consumption (immediately after formation) to form IPNTA of the desired composition $Nb_3W_3O_{19}^{5-}$. This is possible, because with an increase in niobium content in IPNTA the acidity (Z) of their formation also decreases, and becomes similar to Z value for IPTA formation. Third, in concentrated solutions with $c^0_{Nb+W} = 10$ mmol/L the formation of the aprotic form $Nb_3W_3O_{19}^{5-}$ was not witnessed (by the absence of the peak that corresponds to the aprotic form in the diagram), but protonated ions $H_xNb_3W_3O_{19}^{(5-x)-}$ ($x = 1$–3) immediately accumulate, which is in agreement with the tendency of the particles to be protonated in concentrated solutions due to the decrease in the association degree, and, according to ΔG^0_{react}, is thermodynamically more feasible. Besides, protonation is most probably required to stabilize IPNTA with relatively high negative charge.

Based on the distribution diagrams of the studied systems at $c^0_{Nb+W} = 10$ mmol/L, solid phases were isolated in the regions of $H_xNb_3W_3O_{19}^{(5-x)-}$ domination. The content of $HNb_3W_3O_{19}^{4-}$ ($Z_{theor} = 1.00$) at acidity $Z = 1.00$ is ~61 mol.%; at $Z = 1.18$ the contents $H_2Nb_3W_3O_{19}^{3-}$ ($Z_{theor} = 1.18$) is ~70 mol.%. At these Z values thallium and calcium salts were prepared.

All the obtained salts of IPNTA were studied by SEM and EDX and proved to be monophase. Since the morphology of the investigated salts appeared to be similar, the detailed description is exemplified on the individual calcium salt $Ca_{1.5}H_2Nb_3W_3O_{19}\cdot 12H_2O$. Its surface at 1000× magnification consists of the thin flat flakes of the irregular form >10 μm each (Fig. 4*a*). At higher magnification (Fig. 4*b*) aggregates of less than 10 μm that consist of poorly shaped particles with the molten edges (>0.5 μm) can be seen.

Uniform distribution of elements, as presented in Fig. 5*a–e* in backscattered electrons images, as well as the absence of segregations and liquations indicated that the samples were monophase. EDX data for selected areas and individual spots of $Ca_{1.5}H_2Nb_3W_3O_{19}\cdot 12H_2O$ surface (Fig. 6) are summarized in Table 3.

The results above are typical for all the samples under investigation and indicate that the ratio Nb:W = 3:3 is the same in all the sample area and/or spot, and corresponds well to the chemical analysis data (Table 4).

Thallium salts with the anion $H_xNb_3W_3O_{19}^{(5-x)-}$ ($x = 1, 2$) can be assigned to the mixture of salts that contain an anion with Nb:W = 3:3 and various degree of protonation (Table 4), whereas calcium salt of diprotonated IPNTA appeared to be the individual compound (Table 4). For this particular sample an attempt to identify the anion by its FT–IR spectrum has been taken. However, the spectrum turned out to be poorly defined. The most probable reason is that

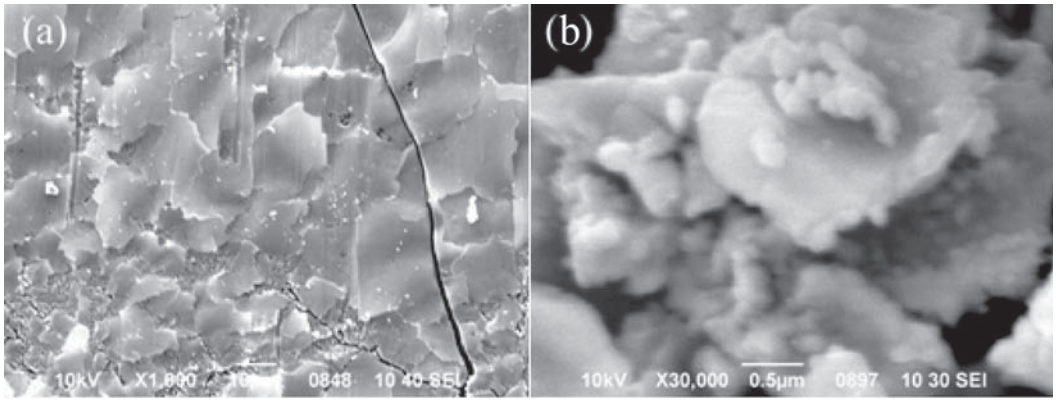

Fig. 4. SEM surface morphology of $Ca_{1.5}H_2Nb_3W_3O_{19}\cdot 12H_2O$ powder. Magnification is *a*) 1000×, and *b*) 30000×

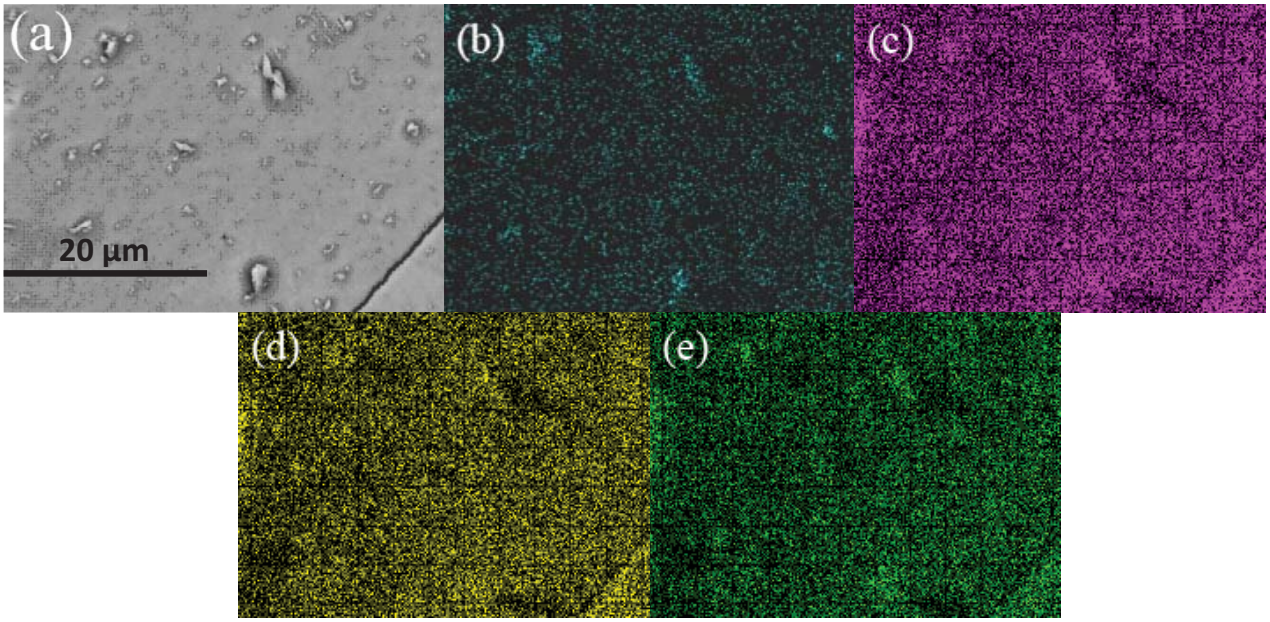

Fig. 5. SEM morphology of $Ca_{1.5}H_2Nb_3W_3O_{19}\cdot 12H_2O$ (*a*). Characteristic radiation *b*) O k_α, *c*) Ca m_α, *d*) Nb l_α, *e*) W m_α. Scalebar is the same for all the images

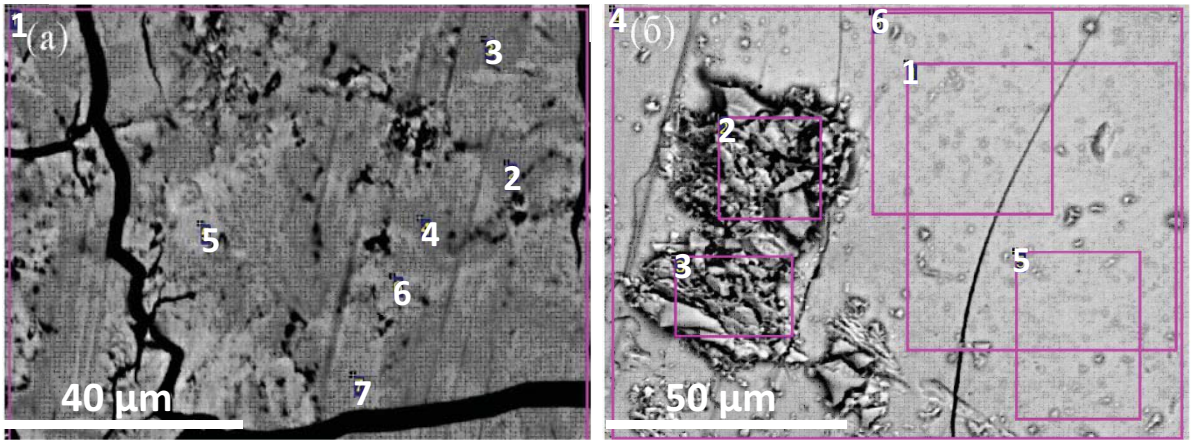

Fig. 6. SEM morphology of $Ca_{1.5}H_2Nb_3W_3O_{19}\cdot 12H_2O$ showing specific areas and spots where EDX data were collected

most of the inorganic cations of IPNTA (including ones from the present study) form X–ray–amorphous hydrates with the well developed network of hydrogen bonds. Thus, to determine the position of characteristic adsorption bands in poorly-defined regions of FTIR spectra they were treated by Peak Fitt plug-in for Origin 8.0 software.

The position and intensity of the main adsorption bands for $Ca_{1.5}H_2Nb_3W_3O_{19}\cdot 12H_2O$ are summarized in Table 5. The most intensive band at 766 cm^{-1} is identical to one in Ref. 26, however, although other bands that correspond to M–O–M vibrations are shifted somewhat to the shorter wave region, we can conclude that the anion in the isolated calcium salt correspond to Lindqvist structural type, which is characteristic for all the IPNTA of the 6th row of Periodic Table.

Identity of IPNTA in solution and in the solid phase of the isolated salts, according to the thermodynamic probability (ΔG^0_{react}) of the possible reactions, allows describing of the processes that take place at acidification of the systems with Nb: W = 3:3 by the scheme of anionic transformations (Scheme).

Table 3. Molar ratio Nb:W in selected spots and areas (Fig. 6) for the powder of $Ca_{1.5}H_2Nb_3W_3O_{19}\cdot 12H_2O$

Fig. 6 (*a*)	ν_{Nb}	ν_W	Fig. 6 (*b*)	ν_{Nb}	ν_W
area 1	3	3.05	area 1	3	2.88
spot 2	3	2.84	area 2	3	2.79
spot 3	3	2.79	area 3	3	3.21
spot 4	3	3.21	area 4	3	3.02
spot 5	3	2.98	area 5	3	2.86
spot 6	3	3.2	area 6	3	3.09
spot 7	3	3.12			
Average for all	3	3.03	Average for all	3	2.98

Table 4. Chemical analyses data for calcium and thallium salts of the obtained IPNTA

Z = 1.00	Tl_2O	Nb_2O_5	WO_3	H_2O
Found, %	34.68	19.18	35.84	11.63
Calcd for $0.42Tl_4HNb_3W_3O_{19}\cdot 12H_2O$ + + $0.58Tl_3H_2Nb_3W_3O_{19}\cdot 13H_2O$, %	35.09	19.38	33.80	11.74
Z = 1.00	CaO	Nb_2O_5	WO_3	H_2O
Found, %	6.06	28.46	49.41	16.42
Calcd for $Ca_{1.5}H_2Nb_3W_3O_{19}\cdot 12H_2O$, %	5.96	28.23	49.24	15.31
Z = 1.18	Tl_2O	Nb_2O_5	WO_3	H_2O
Found, %	28.71	21.66	37.53	10.99
Calcd for $0.54Tl_3H_2Nb_3W_3O_{19}\cdot 13H_2O$ + + $0.46Tl_2H_3Nb_3W_3O_{19}\cdot 7H_2O$, %	29.05	21.81	38.05	11.08
Z = 1.18	CaO	Nb_2O_5	WO_3	H_2O
Found, %	4.66	28.55	50.89	15.90
Calcd for $0.32Ca_{1.5}H_2Nb_3W_3O_{19}\cdot 12H_2O$ + + $0.68CaH_3Nb_3W_3O_{19}\cdot 11.5H_2O$, %	4.67	28.61	49.91	15.08

Table 5. Adsorption bands (cm^{-1}) and their relative intensity (%) in FT–IR spectra of the salts with Nb:W = 3:3 after resolving (vs – very strong, s – strong, m – medium)

Vibration	Nb_3W_3 c Na^+. Cs^+ [27]		$Ca_{1.5}H_2Nb_3W_3O_{19}\cdot 12H_2O$	
	cm^{-1}	%	cm^{-1}	%
M – O – M	522	m	517	12.0
	565	s	612	25.3
	768	vs	766	30.6
	880, 898	s	846	14.1
Nb=O	930	s	885	3.6
W=O	950	s	951	4.5

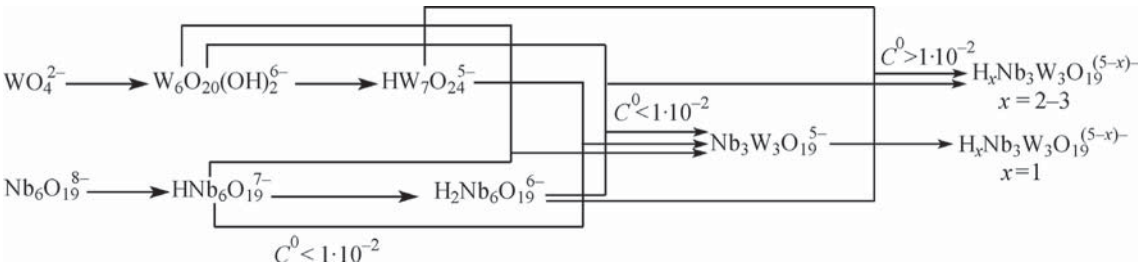

Scheme. Formation of complex anions in the system with Nb:W = 3:3

CONCLUSIONS

Using pH-potentiometric titration and mathematical modeling, the processes of formation of the anions $H_xNb_3W_3O_{19}^{(5-x)-}$ (x = 0–3) in acidified solutions of niobotungstate systems were studied and it has been shown that the targeted IPNTA's (Nb:W = 3:3) form exclusively via the transformation of tetrahedral WO_4^{2-} into $HW_7O_{24}^{5-}$ and/or $W_6O_{20}(OH)_2^{6-}$, possessing octahedral coordination of tungsten by oxygen, followed by interaction of the latter with octahedral coordinated hexaniobate-anions. Noteworthy, IPNTA's with Nb:W = 3:3 form as a result of direct interaction between polytungstate and polyniobate anions without formation of IPNTA's with any other Nb:W ratii, unlike ones with Nb:W = 1:5 and Nb:W = 2:4. Calculations of the thermodynamic parameters ($\Delta G°$) of the studied reactions indicate that they proceed through parallel consecutive schemes. Distribution diagrams of anionic forms in $Nb_6O_{19}^{8-}$–WO_4^{2-}–H^+–H_2O solutions allowed developing of the optimized synthetic procedure towards $Ca_{1.5}H_2Nb_3W_3O_{19}\cdot 12H_2O$ and $Tl_{5-x}H_xNb_3W_3O_{19}\cdot nH_2O$ (x = 1–3) omitting utilization of peroxide compounds. This allowed obtaining of the individual compounds with Nb:W = 3:3 that are not contaminated by other forms.

REFERENCES

1. Maestre J. M., Sarasa J. P., Poblet C. Bo. J. M. *Inorg. Chem*., 1998, vol. 37, no. 12, pp. 3071–3077. DOI: 10.1021/ic960222r

2. Bannani F., Thouvenot R., Debbabi M. *Eur. J. Inorg. Chem*., 2007, pp. 4357–4363. DOI: 10.1002/ejic.200700357

3. Kim Gyu-Shik, Zeng Huadong, Neiwert W. A., Cowan J. J., Van Derveer D., Hill C. L., Weinstock I. A. *Inorg. Chem.*, 2003, vol. 42, no. 18, pp. 5537–5544. Available at: https://www.fpl.fs.fed.us/documnts/pdf2003/kim03a.pdf

4. Lopez X., Weinstock I.A., Sarasa C. Bo. J. P., Poblet J. M. *Inorg. Chem*., 2006, vol. 45, no. 16, pp. 6467–6473. DOI: 10.1021/ic060112c

5. Driss H., Boubekeur K., Debbabi M., Thouvenot R. *Eur. J. Inorg. Chem*., 2008, pp. 3678–3686. DOI: 10.1002/ejic.200800235

6. Stein A., Fendorf M., Jarvie T. P., Mueller K. T., Benesi A. J., Mallouk T. E. *Chem. Mater.*, 1995, vol. 7, no. 2, pp. 304–313. DOI:10.1021/cm00050a012

7. Rhule J. T., Hill C. L., Judd D. A. et al. *Chem. Rev*., 1998, vol. 98, no.1, pp. 327–358. DOI: 10.1021/cr960396q

8. Haugsrud R., Norby T. *Nat. Mater.,* 2006, vol. 5, pp. 193–196. DOI:10.1038/nmat1591

9. Kawakami Y., Ikuta H., Wakihara M. *J. Solid State Electrochem.,* 1998, vol. 2, no. 4, pp. 206–210. DOI: 10.1007/s100080050089

10. Thangadurai V., Adams S., Weppner W. *Chem. Mater.,* 2004, vol. 16, no. 16, pp. 2998–3006. DOI: 10.1021/cm031176d

11. Anderson T. M., Rodriguez M. A., Stewart T. A., Bixler J. N., Wenqian Xu., Parise J. B., Nyman M. *Eur. J. Inorg. Chem*., 2008, pp. 3286–3294. DOI: 10.1002/ejic.200800415

12. Tsonev L. *Opt. Mater.* 2008, vol. 30, no. 6, pp. 892–899. http://www.sciencedirect.com/science/article/pii/S0925346707001140

13. Day V. W., Klemperer W. G., Maltbie D. J. *Organometallics,* 1985, vol. 4, no. 1, pp. 104–111. DOI: 10.1021/om00120a018

14. Klemperer W. G., Main D. J. *Inorg. Chem*., 1990, vol. 29, no. 12, pp. 2355–2360. DOI: 10.1021/ic00337a031

15. Day V. W., Klemperer W. G., Main D. J. *Inorg. Chem*., 1990, vol. 29, no. 12, pp. 2345–2355. DOI: 10.1021/ic00337a030

16. Lu Ying-Jie, Lalancette R., Beer R. H. *Inorg. Chem*., 1996, vol. 35, no. 9, pp. 2524–2529. DOI: 10.1021/ic951197c

17. Dabbabi M., Boyer M. *J. Inorg. Nucl. Chem*., 1976, vol. 38, no. 5, pp. 1011–1014. http://www.sciencedirect.com/science/article/pii/0022190276800188

18. Bates R. *pH Determination. Theory and practice.* Khimija, Leningrad Publ., 1968, pp. 94–124 (in Russian).

19. Kholin Y. *Quantitative Physico-Chemical Analysis of Complex Formation in Solutions and on the Surface of the Chemically Modified Silica: Models, Mathematical Methods and their Applications*. Folio, Kharkov Publ., 2000, p. 288 (in Russian).

20. Pitzer K. S., Mayorga G. *J. Phys.Chem*., 1973, vol. 77, no. 19, pp. 2300–2308. DOI: 10.1021/j100638a009

21. Bugaevski A. A., Kholin Y. V., Konjaev D. S., Krasovitski A. V. *Zh. Obshch. Khim.* 1998, vol. 68, pp. 753–757 (in Russian).

22. Meinrath G. *Anal.Bioanal.Chem*., 2002, vol. 374, no. 5, pp. 796–805. DOI: 10.1007/s00216-002-1547-9

23. Spinner B. *Rev. Chim. Miner*. 1968, vol. 5, no. 4, pp. 839–868.

24. Rozantsev G. M., Sazonova O. I. *Russian Journal of Coordination Chemistry*, 2005, vol. 31, no. 8, pp. 552–558. DOI: http://dx.doi.org/10.1007/s11173-005-0135-x

25. Rozantsev G. M., Vavilova S. M., Belousova E. E. *Russian journal of inorganic chemistry,* 2007, vol. 52, no. 9, pp. 1478–1485. DOI: 10.1134/S003602360709029X

26. Vavilova S. M., Kryuchkov M. A., Belousova K. E., Rozantsev G. M. *Acta Chimica Slovenica*, 2010, vol. 57, no. 2, pp. 341–349. Available at: http://acta-arhiv.chem-soc.si/57/57-2-341.pdf

27. Rocchioli-Deltcheff C., Thouvenot R., Dabbabi M. *Spectrochim. Acta*., 1977, vol. A33, no. 2, pp. 143–153. http://www.sciencedirect.com/science/article/pii/058485397780007X

УДК 536.7:546.78

АНАЛИЗ СОСТОЯНИЯ ИЗОПОЛИНИОБОВОЛЬФРАМАТ-АНИОНОВ (NB:W = 3:3) И СИНТЕЗ ИХ СОЛЕЙ ИЗ ВОДНЫХ РАСТВОРОВ

© 2017 С. М. Вавилова[1], М. А. Крючков[2], В. В. Игнатьева[3], Е. Е. Белоусова[4]

[1]Воронежский государственный медицинский университет им. Н.Н. Бурденко, ул. Студенческая, 10, 394036 Воронеж, Россия
e-mail: svavilova@mail.ru
*[2]Department of Chemistry, McGill University, Montreal, Quebec, Canada**
e-mail: maks_ne@yahoo.com
[3]Донецкий национальный медицинский университет им. М. Горького, пр. Ильича, 16, 282003 Донецк, Донецкая Народная Республика
e-mail: ignatyevavictoriya@gmail.com
[4] Донецкий национальный университет, Университетская ул., 24, 83001 Донецк, Донецкая Народная Республика

Received 20.07.2017

Аннотация. Методом pH-потенциометрического титрования изучены процессы комплексообразования в системе $Nb_6O_{19}^{8-}$–WO_4^{2-}–H^+–H_2O с соотношением Nb:W = 3:3 и концентрациях c^0_{Nb+W} =1·10^{-2}; 5·10^{-3}; 2.5·10^{-3}; 1·10^{-3} моль/л. Методом математического моделирования процессов (компьютерная программа CLINP 2.1), протекающих в изучаемых системах, получены концентрационные константы образования смешанных изополиниобовольфрамат-анионов в интервале (фоновый электролит NaCl) и построены диаграммы их распределения. Рассчитаны термодинамические константы образования анионов $H_xNb_3W_3O_{19}^{(5-x)-}$ (x = 0–3) и показано, что они образуются только после поликонденсации исходных ортовольфрамат-анионов. Синтезированы и идентифицированы методом химического, рентгенспектрального микроанализа, сканирующей электронной микроскопии и ИК-спектроскопического анализа кальциевая $Ca_{1.5}H_2Nb_3W_3O_{19}\cdot 12H_2O$ и таллиевые соли $Tl_{5-x}H_xNb_3W_3O_{19}\cdot nH_2O$ (x = 1–3).

Ключевые слова: полиоксометаллаты, изополианион, изополиниобовольфрамат-анион, анион Линдквиста, формирование модельного комплекса в растворе.

* Present address: BioAstra Technologies Inc., 6100 Av. Royalmount, Montreal, QC, Canada H4P 2R2.

Vavilova Svetlana M. – Cand. Sci. (Chem.), Lecture of Scientific and Mathematical Disciplines Department, Voronezh State Medical University named after N. N. Burdenko; ph.: +7(960) 1220157, e-mail: svavilova@mail.ru

Kryuchkov Maksym A. – Ph. D (Chem.), Department of Chemistry, McGill University, Montreal, Quebec, Canada; e-mail: maks_ne@yahoo.com

Ignatyeva Victoria V. – Cand. Sci. (Chem.), Assistant Professor of Pharmaceutical and Medicinal Chemistry Department M. Gorky Donetsk National Medical University, Donetsk People's Republic; ph.: +38(050) 9001116, e-mail: ignatyevavictoriya@gmail.com

Belousova Ekaterina E. – Cand. Sci. (Chem.), Assistant Professor of Inorganic Chemistry Department, Donetsk National University, Donetsk People's Republic; ph.: +38(050) 2958348